

Full-Wave Evaluations of Loading Factors of Small Animal RF Receive Coils

S. Wang¹, S. Dodd¹, and J. H. Duyn¹

¹LRFMI/NINDS/NIH, Bethesda, MD, United States

Introduction: When sample-noise is not the dominating factor, coil noise estimation is important in designing high-Q receive coils. This typically happens when the imaging subject is small, e.g., rodent imaging, or a very large number of elements are sought, e.g., multi-channel head coil array (1). Accurate estimations of coil noise are much desired in guiding the design of coil-noise dominated RF receivers to achieve high SNR. To this end, accurate current distribution on coil surfaces is required (2). We developed a rectangular-element-based integral-equation approach to capture the current distribution on coil surfaces and utilized that information to compute the coil noise. The salient feature is that very small elements, which are required to capture coil current distribution, are confined to coils and do not increase the cost of modeling other parts of a system, e.g., phantoms.

Methods: The surface-integral equation is based on solving current distributions on conductors or phantom surfaces. Surface currents are integrated to obtain vector potentials through Green's function and the radiated electromagnetic fields are calculated thereafter (3). Among the many factors, the major concern of choosing an appropriate integral-equation-based approach in this study is the type of elements being used to expand the current distribution. Since coil cross-section needs to be discretized very finely to capture current distribution, and coil features are usually larger than its cross-section size, rectangular patches are sufficient in geometric modeling. Other advantages of choosing rectangular over triangular elements

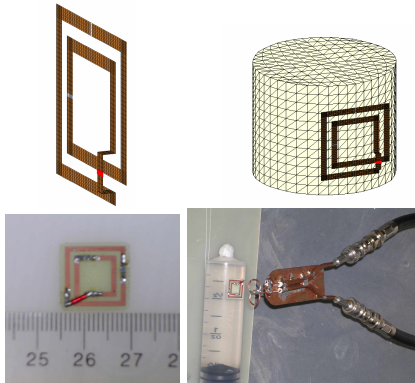


Figure 1: Upper left: coil model, where grey color represents capacitors and red color represents excitation. Upper right: simulation setup for loaded Q. Note that the phantom surface can be modeled by triangular patches of larger sizes. Lower left: 2-turn air-bridged spiral coil. Lower right: experimental set up for measuring loaded Q.

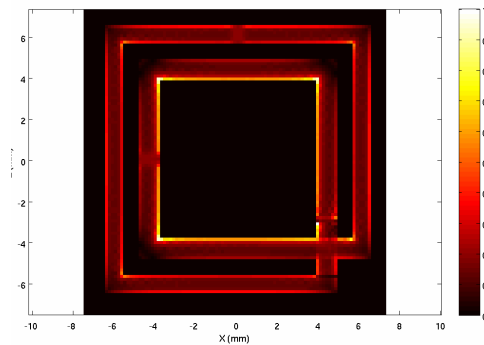


Figure 2: Simulated current distribution on the spiral coil surface. The current mainly flows along the two edges, especially the inner edge of the inner turn. Also, the current is the strongest around the corners.

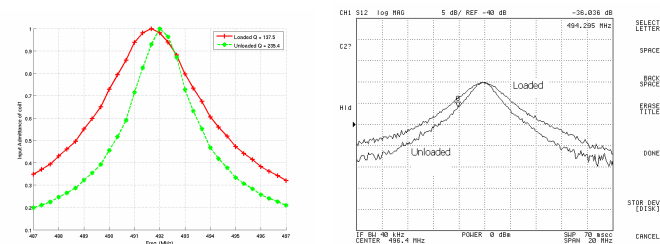


Figure 3: Left: simulated loaded and unloaded Q factors. Right: measured loaded and unloaded Q factors. The wider line is the loaded measurement result, which is aligned with the unloaded one.

	Simulation	Experiment
Capacitor 1	4.3 pF	4.3 pF
Capacitor 2 & 3	5.3 pF	5.6 pF
Unloaded Resonant Frequency	492 MHz	497.4 MHz
Loaded Resonant Frequency	491.67 MHz	495 MHz
Unloaded Q	235.4	222.1
Loaded Q	137.5	121.6
Ratio of loaded and unloaded Q	0.584	0.548

Table 1: Comparison of the simulation and the experiment results.

program to study the loaded and unloaded Q-factors of a two-turn air-bridged spiral coil for rat-brain imaging at 11.7 Tesla (Fig. 1). The outline of the spiral coil is a 1.3 cm by 1.3 cm square. The coil is made of 1-mm wide copper traces and the gaps between parallel traces are also 1-mm wide. The conductivity of copper traces is $5.8e7$ S/m. At one corner, an air-bridge is constructed to form a closed circuit without shorting the coil. Three capacitors are used in coil tuning, one 4.3 pF capacitor collocating with the feeding and two 5.3 pF ones. The Q-factors of the capacitors were found from manufacture's specifications (Voltronics), which are 700 for the 4.3 pF capacitor and 600 for the 5.3 pF ones. A cylindrical phantom filled with 55 milli-molar sodium chloride was used to load the coil. A spiral coil was manufactured for measurements accordingly (Fig. 1). The coil was milled to an accuracy of within 0.1 mm. We avoided the use of low Q trimmer capacitors, using only available fixed capacitors, and finding a combination which achieved a resonant frequency as close as possible to 500 MHz. Nine elements across the coil cross-section were used for capturing current distribution. The simulated current distribution is shown in Fig. 2. In general, current primarily flows along the inner edges and is the strongest around corners. Figure 2 shows both the simulated and the experimental resonant curves of the loaded and unloaded coils. The Q factors can be calculated from these curves and the results are summarized in Table 1. The simulation results, especially the loaded/unloaded Q factor ratios, are very close to the measurements. The difference between the measured and simulated Q factors may be mainly contributed to the substrate loss in the unloaded case and the syringe wall loss in the loaded case. Both are unaccounted for in simulations due to the lack of relevant specifications.

Conclusion: We developed an integral-equation-based approach for simulating coil-noise dominated small animal RF coils. Experiment results show the validity and accuracy of the approach. It would also be useful in designing human coil arrays with very large number of channels.

References: 1) Patrick et al, ISMRM, Seattle, 2006 p. 422. 2) Tulyathan, P. et al, IEEE Trans. AP, 27:46-49, 1979. 3) R.F. Harrington Field computation by method of moments. IEEE Press.